

## 3D CONE-BEAM TOMOGRAPHY FOR NON-DESTRUCTIVE TESTING

Per-Erik Danielsson  
Image Processing Laboratory  
Department of Electrical Engineering, Linköping University

S-581 83 LINKÖPING, Sweden  
email: ped@isy.liu.se

### ABSTRACT

Many new imaging technologies have evolved in the aftermath of computerized tomography (CT). In the field of non-destructive testing (NDT) the CT-machines are mostly extensions of instruments for digital radiography. In contrast to medical CT-machines the NDT-versions rotate the object instead of the gantry, utilize the magnifying power of the X-ray point projection system, and are equipped with a 2D-detector. Hence, utilizing a cone-beam for 3D-reconstruction instead of a fan-beam is an inviting possibility. In addition, the cone-beam is utilizing the X-ray source much more efficiently.

The dominating reconstruction technique is filtered back-projection, at which a non-exact 3D-version was proposed by Feldkamp et al. An exact 3D-reconstruction requires that the full Radon space should be retrieved or computed, i.e. values for integrals over planes through the object. One such method was developed by Grangeat having the computation complexity  $O(N^4)$ . The direct Fourier method in the linogram version has been shown to preserve full image quality. In a 3D-case it has then been possible to implement the Grangeat method with  $O(N^3 \log N)$  complexity.

Exact reconstruction requires special source trajectories; a single circular scan around the object is not sufficient. Missing data may be compensated for in case there is data available for a golden part. Most if not all NDT-cases would benefit from the possibility to highlight (focus) on a subvolume inside the whole object. Physical constraints such as beam-hardening and scattering may in the end be the most severe limitations to 3D-cone-beam tomography for NDT.

### STATE-OF-THE ART IN TOMOGRAPHY

Computerized tomography (CT) is a prime example of a technological break-through. Besides being a global success of its own, CT spawned wide-spread interests in new imaging techniques. Indirectly, Magnetic Resonance imaging (MR), Positron-Emission Tomography (PET) and many other modalities are descendants of this global success which showed that the physical probe does not necessarily have to produce an image directly. As long as the data acquisition is complete the image may well lie

hidden in this data set waiting for development by a numerical process which is known as **reconstruction** but called **inversion** by the mathematicians.

To acquire new images from nature beats everything in science and engineering. In fact, modern science did not take off until the telescope and the microscope were invented some 300 years ago. Likewise, in more modern times several Nobel prizes have been awarded in imaging technology: Röntgen 1903, Ruska (electron microscopy) 1986, Zernike (phase contrast microscopy) 1953, Gabor (holography) 1971, Klug (el. microscopy) 1982, Hounsfield and Cormack (CT) 1979, Binning and Rohrer (tunnel microscopy) 1986. Intensive research and developments continue all over the world in MR, PET, confocal microscopy and many other fields.

The dominating application for CT is of course to examine the human body. The most modern machines have the following typical performance numbers and characteristics.

- Fan-beam  $\pm 30^\circ$ .
- 800 detectors along a circular arc
- Slip ring to allow for spiral source-path
- Reconstruction using filtered back-projection
- Reconstructed image size: 512x512 pixel
- Reconstruction time: 1 sec.

3D-volumes still have to be reconstructed slice-by-slice, but the slip-ring (which supports all connections to the rotating gantry) has made 3D CT-volumes more easily accessible. Acquisition speed is still a problem as is the limited axial resolution compared to the in-slice resolution. The standard reconstruction method is filtered backprojection which requires approximately 1 GFLOP (Giga Floating Point Operation) for the image size 512x512. Necessary computation speed is achieved with semi-custom "back-projection boards".

For non-destructive testing (NDT) of small to medium sized objects the tomograph can be designed quite differently from the medical case. See Figure 1. The object is mounted on a turn-table which can be translated in all three coordinates. Thus, instead of letting the X-ray source and the detector rotate around the patient, we turn the object itself.

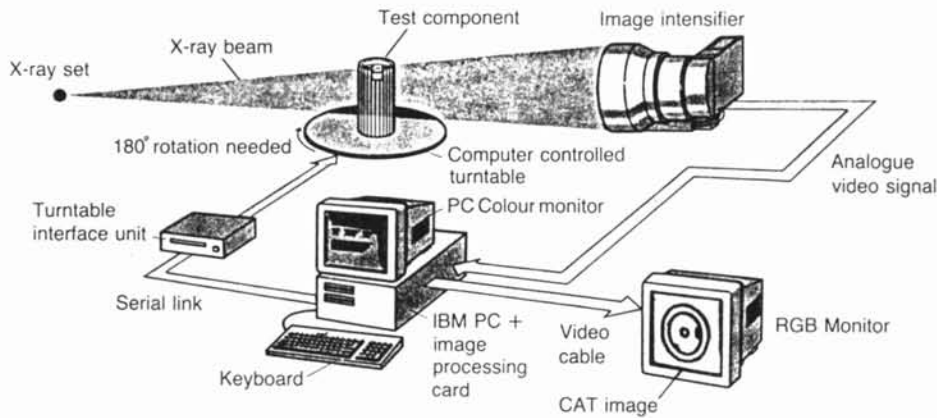


Figure 1

These machines are all descendants or rather augmentations of digital radiography. The detector system consists of an image intensifier followed by an optical link which maps the projection image on a CCD-array. Cooling and slow read-out makes it possible to get 12 significant bit accuracy from a 1024x1024 array at one frame/sec. For medical CT this accuracy is not sufficient but for NDT the density contrast in the object is high enough to compensate for less accurate detector data. The image intensifier presents other problems, however. One of these is heavy geometric distortion which has to be calibrated and corrected for. In spite of its problems, the image intensifier is today the only viable and practical 2D-detector of reasonable size. The hunt is on to find an alternative, mostly behind closed doors in proprietary laboratories.

Contrary to medical CT-machines, the tomograph in Figure 1 is able to **magnify**. Small objects are placed close to the X-ray source and the cone-shaped beam of photons creates a 2D point projection of the object onto the detector plane. As long as the object does not collide with the X-ray source during rotation and its longest diameter does not fall off the image frame any geometric magnification is acceptable. The **resolution** of the detector system is limited by the digital resolution in the detector but also the size of the X-ray focus. The latter can be made small but at the expense of excessive concentrated heating at a small spot of the X-ray tube target (the anode) or, alternatively, a reduced number of photons in the cone-beam.

The 2D-detector in systems like the one in Figure 1 is potentially ready to be used for 3D-reconstruction from 2D-projections but rather few are used in this way. Instead one or a few parallel slices close to the midsection of the source-detector system are reconstructed from a sequence of a set of parallel detector lines. For low magnifications the beam is only mildly divergent and these lines may then all be considered as receiving a set of parallel fan-beam projections.

As of today, only highly precious and precarious components have been subjected to NDT with X-ray CT on a more regular basis. Among these are turbine blades for aircraft engines, composite materials in critical industrial parts, and certain types of military ammunition.

### RECONSTRUCTION WITH FILTERED BACK-PROJECTION

Filtered back-projection is a transform method. Like all such methods it is based on the Fourier slice theorem which is illustrated in Figure 2. A set of parallel projection data taken at angle  $\phi + \pi/2$  is equivalent to a set of line integrals through  $f(x, y)$ . (The fan-beam case is possible to treat in a similar fashion). These line integrals are by definition

the Radon transform  $\mathcal{R}$

$$\mathcal{R}f(\rho, \phi) = \int_{-\infty}^{\infty} \int_{-\infty}^{\infty} f(x, y) \delta(x \cos \phi + y \sin \phi - \rho) dx dy \quad (1)$$

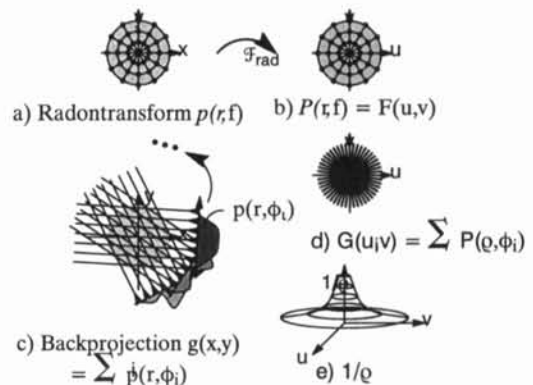


Figure 2

where  $q$  is the distance from the origin to the line of integration. The Fourier slice theorem then tells us that the one-dimensional Fourier transform of a projection (a slice of Radon transform data) becomes a slice of data in the 2D Fourier transform of  $f(x, y)$ , i.e.

$$\mathcal{F}_{\text{rad}} \mathcal{R} f = \mathcal{F}_2 f \quad (2)$$

Backprojection is equivalent to use each slice of the Radon transform as an image having constant values along the lines of integration. These images are summed. Observing the Fourier domain in Figure 2 d) e) we notice that the result is a heavy overemphasis of the low frequency content in the original object function  $f(x, y)$ . Hence, this inherent low-pass filter in the projection-backprojection procedure has to be compensated by a high-pass filter (ideally a rampfilter).

The computation expense is dominated by the back-projections. Each of the  $N \times N$  pixel in the result is to receive and accumulate a contribution from each of the  $O(N)$  filtered projections. Hence the complexity is  $O(N^3)$ .

As mentioned, a 3D-volume may be reconstructed as a sequence of 2D-slices. Seen as a measurement and data acquisition task this is highly inefficient, however. Any X-ray source produces photons in a cone-beam and the fan-beam system for 2D-reconstruction is wasting the majority of these measurement probes in the collimator as illustrated in Figure 3. The waste has to be made up for by longer integration time per detector value and/or lower signal to noise ratio.

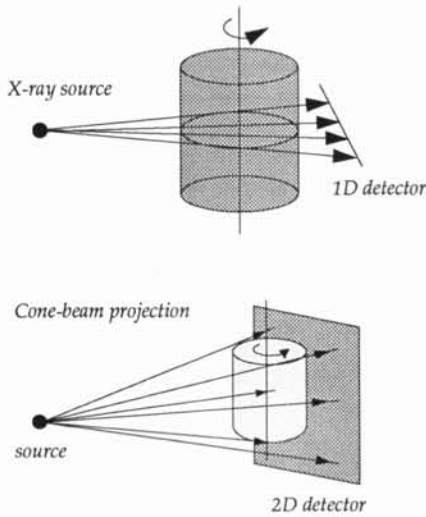


Figure 3

Exploitation of the full cone-beam was first proposed by Feldkamp et al [1] and their reconstruction technique has become somewhat of standard in NDT-applications. The Feldkamp algorithm is a seemingly straight-forward generalization of 2D-filtered back-projection. See

Figure 3. Each horizontal line of projector data retrieved from the cone-beam projection is filtered in very much the same manner as if it were an in-slice fan-beam projection in the 2D-case. Then, the filtered data are back-projected into the 3D-volume along the ray paths known a priori.

The reconstruction result is not exact in the mathematical sense. That is, apart from all practical aspects, approximations, noise, geometrical limitations, etc, the reconstructed 3D density function will differ from the real object even if the detector had an infinite number of source positions. Object details along the plane of the circular source orbit are reconstructed exactly but the artefacts increase with increasing cone-beam angle.

A comparative study of 3D-reconstructions have been performed [2] where the following 3D reconstruction techniques were implemented.

- i) Parallel slice assumption as mentioned above in connection with Figure 1.
- ii) The Feldkamp method.
- iii) The Grangeat method.

For  $128^3$  resolution we interpret the results as follows. For "reasonable" image quality and freedom of artefacts the method i) works for cone-beam angles  $\pm 0.5^\circ$ , the Feldkamp method for  $\pm 5^\circ$ , the Grangeat method for  $\pm 9^\circ$ . With complete data capture, however, the Grangeat method works for any cone-beam angle as will be shown below.

### AN EXACT CONE-BEAM ALGORITHM

According to Natterer [3] the inversion formula for the 2D-case can be written

$$f(\vec{r}) = \frac{1}{2} \frac{1}{2\pi} \int_{-\pi}^{\pi} \frac{1}{\pi q} * \frac{\partial}{\partial q} \mathcal{R} f(q, \phi) d\phi \quad (3)$$

Here, the Hilbert transform kernel  $1/4\pi^2 q$  convolved with the derivative operator yields exactly the convolution kernel which corresponds to the well-known rampfilter in the Fourier domain. The 3D-version of (3) is

$$f(\vec{r}) = \frac{1}{2} \left( \frac{1}{2\pi} \right)^2 \int_{S^2} (-1) \frac{\partial^2}{\partial q^2} \mathcal{R} f(q, \theta) d\theta \quad (4)$$

where  $q$  is now a 3D-vector in the 3D-Radon space where each point represents a *plane integral* over the object space. The angle  $\theta$  is a 2D-angle on the unit sphere (commonly denoted with the pair  $\theta, \phi$ ). This unit sphere  $S^2$  is also the domain of integration just as the unit circle is the domain of integration in the 2D-case. We notice that the rampfilter kernel in (3) is reduced to a plain second derivative in (4). Equation (4) may be interpreted as a recipe for reconstruction by which each filtered Radon data should be back-projected to all points in the plane from where it originated.

The obvious question is: How can we get plane integrals from X-ray data which only represent line integrals? If the 2D-detector data represent a parallel projection things are easy. Any line in the detector plane then defines a plane through the object. Summing data along this line yields a plane integral. The cone-beam projection is different. Summing along a line in the detector plane does not yield a plane integral.

Fortunately, Grangeat has shown [4], that the derivative of the Radon transform is retrievable from cone-beam data. See Figure 4. Without loss of generality we place the (virtual) detector plane vertically through the object  $f$ . The detector harbors line integrals through the object  $Xf$ . A line of integration  $t$  in the detector plane defines a plane of integration, a Radon plane through the X-ray source  $S$ . The normal from origin  $O$  to this arbitrary plane is the 3D-vector  $\varrho$  and we write the Radon value for this plane as follows.

$$\mathfrak{R}f(\varrho) = \int_{-\pi/2}^{\pi/2} \int_0^{\infty} f(\varrho, r, \gamma) r \, dr \, d\gamma \quad (5)$$

Line integrals (detector data) in the  $\gamma$ -direction are described by

$$Xf(\varrho, \gamma) = \int_0^{\infty} f(\varrho, r, \gamma) \, dr \quad (6)$$

From Figure 4 b) and 4 c) we have

$$d\varrho(r) = d\beta \, r \cos\gamma \quad (7)$$

$$SC \, dy = \cos^2\gamma \, dt \quad (8)$$

$$SC = SA \cos\gamma \quad (9)$$

$$SO \, d\beta = \cos^2\beta \, ds \quad (10)$$

The derivative of (5) using (6), (7), (8), (9) and (10) becomes

$$\begin{aligned} \frac{d}{d\varrho} [\mathfrak{R}f(\varrho)] &= \int_{-\pi/2}^{\pi/2} \int_0^{\infty} \frac{d}{d\beta} f(\varrho, r, \gamma) \frac{1}{\cos\gamma} \, dr \, d\gamma = \\ &= \frac{d}{d\beta} \int_{-\pi/2}^{\pi/2} Xf(\varrho, \gamma) \frac{1}{\cos\gamma} \, d\gamma = \\ &= \frac{SO}{\cos^2\beta} \frac{d}{ds} \int_{-\infty}^{\infty} \frac{1}{SA} Xf(\varrho, t) \, dt \quad (11) \end{aligned}$$

This is (one formulation of) Grangeat's result. From inside out (11) gives the following recipe for computing the first derivative (in the radial direction) of the Radon transform of  $f$ .

- i) Weight the detector data with the factor  $1/SA$ , where  $SA$  is the distance to the source  $S$ .
- ii) Integrate detector data along the intersection line between the detector plane and the wanted Radon value plane.
- iii) Take the derivative in the  $s$ -direction (in the detector plane perpendicular to the integration line).
- iv) Weight the 2D data set resulting from one single source position with the factor  $SO/\cos^2\beta$ .

In [4] the line integration ii) and the derivative computation iii) for the  $O(N^2)$  points in a detector plane is performed with an  $O(N)$  procedure so that the total computation of Radon derivative values in  $O(N)$  detector planes is rendered the complexity  $O(N^4)$ .

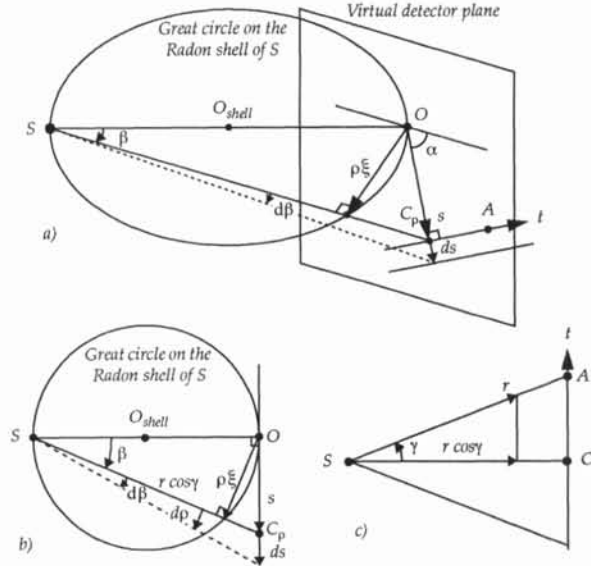


Figure 4

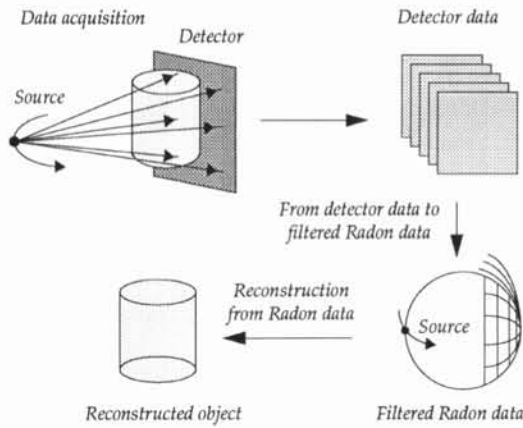


Figure 5

Thus, as indicated in Figure 5, the total procedure due to Grangeat consists of two distinct phases. In the first one we convert the set of detector data to Radon data, i.e. to derivative of integrals over planes in the object. In the second phase, Radon data are used to reconstruct the object, not necessarily using the sampling indicated in Figure 5. In fact, following an idea by Marr [5], Grangeat in his work performed the reconstruction in two steps.

The first of these steps assumes that Radon data are resampled at points which are situated on vertical planes, all of them going through the  $z$ -axis but having different rotation angle. For each such plane ordinary 2D-reconstruction is performed which brings about a result which represents a set of parallel line integration values through the object. Hence, by assembling a horizontal set of these from each vertical plane we have for each horizontal plane the necessary set of line integrals for 2D-reconstruction of horizontal planes of the object itself. This is the second step of the reconstruction phase. Using filtered back-projection the  $O(N)$  horizontal planes are all reconstructed with an  $O(N^3)$  procedure. Thus, the second phase, from Radon data to object data, is also of complexity  $O(N^4)$ .

#### FOURIER METHODS. LINOGRAMS.

It is common knowledge that the so called direct Fourier method is inherently faster than filtered backprojection. In fact, the first paper using this technique was published by Tretiak and Eden in 1969 [6]. The principle is illustrated in Figure 6 and builds directly on the Fourier slice theorem (2). The projections, i.e. the Radon data, are brought to the Fourier domain just as in Figure 2. However, instead of summing these we are using them for resampling (interpolation) the Fourier domain into a Cartesian grid. An inverse 2D Fourier-transform brings about the final reconstructed result.

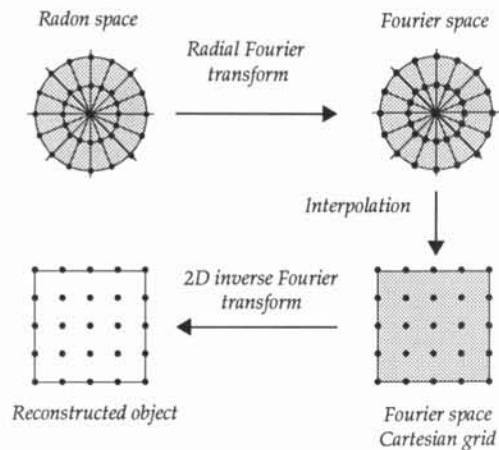


Figure 6

It is easy to see that by using FFT-operations, the complexity of the operations in Figure 6 is  $O(N^2 \log N)$ . In spite of this advantage in speed, the direct Fourier method has been shunned in practice because of its alleged lower image quality. Usually, the Fourier domain interpolation is pointed out as the culprit.

However, there are now accumulative evidence that these problems can be overcome [7], [8], [9]. As shown in [9] there are two problems with the direct Fourier method. One of these is indeed the highly critical interpolation. The other one is an *implicit* inherent high pass filtering with a ramp filter. This will cause circular convolution in the Fourier domain unless special precautions are taken in the form of truncation of the convolution kernel and zero-padding the image function. In the Fourier domain, this corresponds to a modified ramp filter and double sampling density, respectively.

The *linogram* technique for image reconstruction was proposed by Edholm [10] and further developed and implemented by Magnusson for the 2D-case [11] and by Axelsson for the 3D-case [12]. The method may conveniently be portrayed as a direct Fourier method with an unconventional sampling pattern for the Radon space. See Figure 7. The samples are aligned along radial lines just as in Figure 6 but not along concentric circles. Instead, we identify four lobes where the samples are positioned on circular arcs.

The virtue of this sampling pattern comes forward in the Fourier domain. We arrive there from the Radon space as before using 1D Fourier transforms of data positioned along radial lines. In the Fourier domain the samples are now equidistantly located on concentric squares. This sampling pattern is much more regular with respect to the Cartesian grid than the circular symmetric pattern in Figure 6 so that only 1D-interpolation is needed. In fact, using the so called Chirp  $z$  transform, no interpolation is

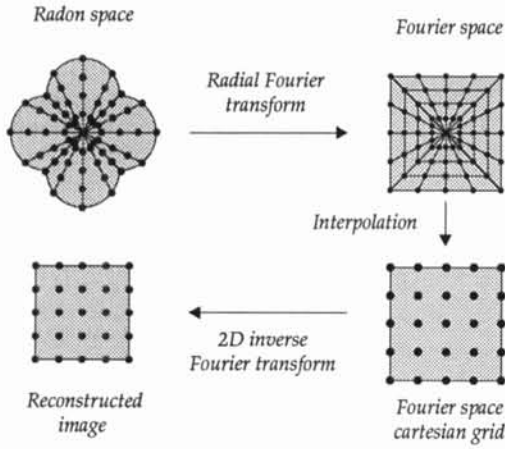


Figure 7

needed at all. The Chirp z transform is more complicated than FFT but retains the basic  $O(N \log N)$  complexity [12].

For the 3D-case, Figure 5, the Fourier-linogram technique may be employed in both phase 1 and phase 2 [13]. We notice that the most burdensome of the tasks in the first phase was line integration in the detector plane. However, this is equivalent to computing the Radon transform and we may then use (2) again, this time in the form

$$\mathcal{R}f = \mathcal{F}_{\text{rad}}^{-1} \mathcal{F}_2 f \quad (12)$$

Thus, the implementation of (11) may then be done as shown in Figure 8 and the complexity is hereby brought to  $O(N^3 \log N)$ . The corresponding reduction of complexity

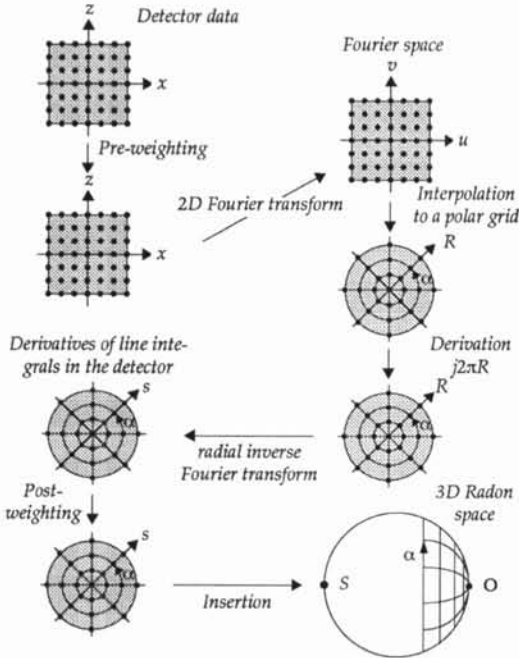


Figure 8

for phase two follows directly from the fact that it consists of  $O(N)$  2D-reconstructions, each having the complexity  $O(N^2 \log N)$  when applying direct Fourier techniques.

In [12], Axelsson has shown that under reasonable assumptions, the Fourier techniques should win in speed over the original implementation of the Grangeat algorithm with a factor of 10 for a  $512 \times 512 \times 512$  volume. However, this remains to be validated in a practical implementation.

### LINGERING PROBLEMS FOR 3D CT

From Figure 4 it is possible to infer that from one single source position  $S$ , all obtainable Radon data are situated on a sphere, the Radon shell of  $S$  which has  $SO$  as a diameter. Because of the finite extension of the detector, the shell is partly empty, truncated into umbrella-like surfaces which form the result of the first phase of Grangeat's method [4]. Neglecting this truncation effect, a full set of Radon data from a circular source trajectory is shown in Figure 9. It is easy to see that no Radon data are retrievable in the vicinity of the z-axis. If the object is small compared to the distance  $SO$  (small cone-beam angles) the missing volume may be negligible, for larger cone-beam angles the missing data section is bound to have a detrimental effect on the reconstructed result.

The role of these *missing data* may be understood by applying the 3D Fourier slice theorem to Figure 9. Each radial line of data in Figure 9 may be 1D Fourier transformed to contribute to the 3D Fourier transform of the object. But because of missing Radon data, near the z-axis the Fourier space will be empty or incomplete just as the Radon space.

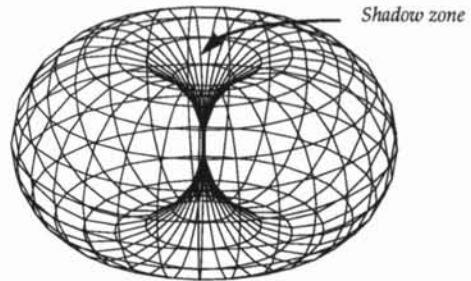


Figure 9

One remedy to this situation is to augment the horizontal circular source trajectory with a vertical one. The Radon space of the object will then be fully covered by one or by both trajectories. Actually, the dual circle is only one of several possible trajectories. Another one is to move the source (and the detector) on a spiral-like curve or a sphere as indicated in Figure 10. In the NDT-case (Figure 1) we may implement this by mounting the object on one tilted axis, the platform of which is rotated around a vertical axis.

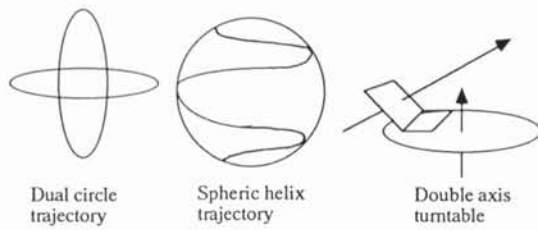


Figure 10

The combined incremental rotations around the two axes will make it possible to expose the object from almost every angle and avoid any missing data of the type shown in Figure 9.

In many applications of inspection and quality control the sheer size and extension prohibit the use of a tomograph of the type shown in Figure 1. Therefore, a complete plane integral may be inaccessible even for planes which pass through the source position. This is to say that some data on the Radon shell itself are *incomplete* and will produce artifacts in the reconstructed result.

This situation can only be handled by using extra a priori information. In many NDT-applications a "golden part" is available. Projection data are taken from the golden part under the same restriction as for the part under examination. Corresponding projections are then subtracted from each other and the difference is used for reconstruction. The difference image is not perfect but in many cases good enough for flaw indication and localization.

In many cases, one would like to focus the reconstruction to a small subvolume somewhere inside the object, a *region-of-interest*. In fact, one of the draw-backs of medical CT is the limited resolution (approx. 1 mm). It should be of tremendous importance if it would be possible to reconstruct a smaller part of the human body, e.g. a damaged vertebra, with higher resolution without increasing the resolution of the detector system correspondingly. For the medical CT no good solution seems to exist. For the NDT-machine of Figure 1, however, the following idea should be useful. First we reconstruct the whole object using a magnification which is low enough to make room for the whole object inside the detector. Then we increase the magnification so that parts of the projection of the object falls outside the detector. But since the object is now known, albeit in somewhat lower resolution we may fill in the missing detector data rather satisfactorily and proceed with the high resolution, reconstruction. Actually, it can be shown that one can use the Radon space instead of the object space as a basis for estimation and filling in such high resolution data which cannot be measured because of the limited detector.

The basis for CT is the assumption that the X-rays are moving in straight lines and attenuated according to one

single feature of the material, the attenuation coefficient  $f$ . The reconstructed image is a map of the function  $f(x, y, z)$ . However, these and some other assumptions are only approximately true because the X-ray source is not monochromatic; the X-ray photons have different energies for which the material has different attenuation coefficients. Typically, the high energy photons are less attenuated than the low energy ones and the result is called *beam-hardening*. The ray becomes harder (to attenuate) the further it penetrates the object.

Another phenomenon is *scatter*, which consists of photons which are evoked inside the object by the incoming photons from the source. These secondary photons have a totally randomized direction; they can be envisioned as a glow, some of which will reach the detector. Low-level signals at the detector run the risk of being drowned by this scatter noise.

It should be noted that the scattering problem is much worse in cone-beam 3D tomography than in 2D tomography. In the latter case the primary cone-beam may be collimated into a fan-beam which causes only a small part of the object to glow. The cone-beam causes the whole object to glow. Larger objects that require to be placed close to the detector in Figure 1 may prove to be impossible to reconstruct from cone-beam data due to the unavoidable scatter problem.

#### REFERENCES

- [1] L.A. Feldkamp, L.C. Davis, J.W. Kreiss: *Practical cone beam algorithms*. Journal of Optical Soc. Am., Vol A6, 1984.
- [2] P. Grangeat, P. Le Mason, P. Melennec, P. Sire: *Evaluation of the 3D Radon transform algorithm for cone-beam reconstruction*. SPIE Medical Imaging V, Technical Conference 1445: Image Processing, February 23-March 1, San Jose, California, USA, pp 320-331, 1991.
- [3] Natterer: *The Mathematics of Computerized Tomography*. John Wiley & Sons Ltd and B.G. Teubner, 1986.
- [4] P. Grangeat: *Mathematical framework of cone beam 3D reconstruction via the first derivative of the Radon transform*. Mathematical Methods in Tomography, Herman Louis, natterer (eds.), Lecture notes in Mathematics, Springer Verlag 1991.
- [5] R.B. Marr, C. Chen, P.C. Lauterbur: *On two approaches to 3D reconstruction in NMR zeugmatography*. Proc. of Mathematical Aspect of Computerized Tomography. Oberwolfach (FRG), 1980, ed. by G.T. Herman, F. Natterer, Springer Verlag, 1981.

- [6] O. Tretiak, M. Eden: *Internal structure from X-ray images*. 8th Int. Conf. on Medical and Biological Engineering, Chicago, July 25-29, 1969.
- [7] J.D. O'Sullivan: *A Fast Sinc Function Gridding Algorithm for Fourier Inversion in Tomography*. IEEE Transactions on Medical Imaging, Vol M1-4, No 4, December 1985.
- [8] S. Matej, I. Bajla: *A High Speed Reconstruction from Projections using Direct Fourier Methods with Optimized Parameters. An Experimental Analysis*. IEEE Transactions on Medical Imaging, Vol 9, pp 421-429, 1990.
- [9] M. Magnusson, P.E. Danielsson, P. Edholm: *Artefacts and Remedies in Direct Fourier Tomographic Reconstruction*. Proc. of the IEEE Medical Imaging Conference, Orlando, Florida, October 27-31, 1992, pp 1138-1140.
- [10] P.R. Edholm: *CT algorithms with linograms*. Proc. of the 12th Annual International Conference of the IEEE Engineering in Medicine and Biology Society, Philadelphia, USA, November 1-4, 1990, pp 372-373.
- [11] M. Magnusson: *Linogram and other Direct Fourier Methods for Tomographic Reconstruction*. Linköping Studies in Science and Technology. Ph.D. Thesis No. 320. Dept. of EE, Linköping University, November 1993.
- [12] C. Axelsson: *Direct Fourier Methods in 3D-Reconstruction from Cone-Beam Data*. Linköping Studies in Science and Technology. Licentiate thesis No. 413. Dept. of EE, Linköping University, January 1994.
- [13] P.E. Danielsson: *From Cone-Beam Projections to 3D Radon Data in  $O(N^3 \log N)$  Time*. Proc. of the IEEE Medical Imaging Conference, Orlando, Florida, October 27-31, 1992, pp 1135-1137.